Supplementary for Expediting Large-Scale Vision Transformer for Dense Prediction without Fine-tuning

Weicong Liang[1]* **Yuhui Yuan[4]*†** **Henghui Ding[3]** **Xiao Luo[2]**
Weihong Lin[4] **Ding Jia[1]** **Zheng Zhang[4]** **Chao Zhang[1]** **Han Hu[4]**
[1]Key Laboratory of Machine Perception (MOE)
School of Intelligence Science and Technology, Peking University
[2]School of Mathematical Sciences, Peking University [3]ETH Zurich
[4]Microsoft Research Asia

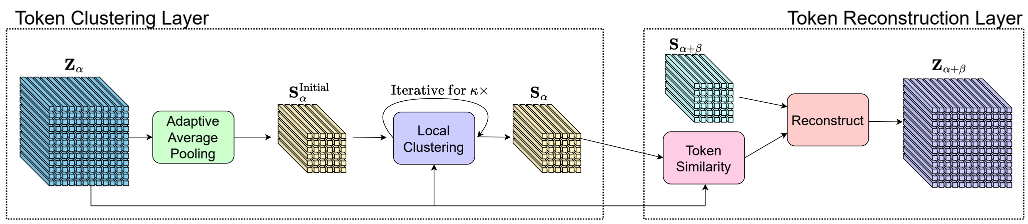

Figure 1: Illustrating more details of our approach. The token clustering layer consists of an adaptive average pooling block (for initializing the cluster centers) and an iterative local clustering block (for performing the k-means clustering). The token reconstruction layer consists of a token similarity estimation block (for estimating the reconstruction relation matrix) and a reconstruction block (for reconstructing the high-resolution representations). $\mathbf{Z}_\alpha$ represents the original high-resolution representations after α-th transformer layer. $\mathbf{S}_\alpha$ represents the clustered low-resolution representations by token clustering layer. $\mathbf{S}_{\alpha+\beta}$ represents the refined clustered low-resolution representations after additional β transformer layers. $\mathbf{Z}_{\alpha+\beta}$ represents the reconstructed high-resolution representations from $\mathbf{S}_{\alpha+\beta}$ by using the token reconstruction layer.

A. Illustrating More Details of Our Approach

We first illustrate the overall details of our token clustering layer and token reconstruction layer in Figure 1. We then present the example implementation of token clustering layer and token reconstruction layer based on PyTorch in Listing 1 and Listing 2, respectively.

B. More Hyper-parameter Details

We summarize the detailed hyper-parameter settings for the dense prediction methods based on plain ViTs and Swin Transformers in Table 1 and Table 2, respectively.

Table 1 summarizes the hyper-parameters, including the inserted positions α & α+β of token clustering layer & token reconstruction layer, the number of remaining transformer layers after the token reconstruction layer γ, the total number of transformer layers L, the number of tokens before clustering $\frac{\mathsf{H}}{\mathsf{P}} \times \frac{\mathsf{W}}{\mathsf{P}}$, the number of tokens after clustering $\mathsf{h} \times \mathsf{w}$, the number of neighboring pixels λ, the number of EM iterations κ, the temperature value τ, and the number of nearest neighbors k, for Segmenter, DPT, and SWAG.

*Equal contribution.
†✉ yuhui.yuan@microsoft.com

36th Conference on Neural Information Processing Systems (NeurIPS 2022).

```python
def token_clustering_layer(features, cluster_features_shape, num_iters, tau):
    # args:
    #       features: shape [B, C, H, W]
    #       cluster_features_shape: [h, w]
    #       num_iters: num of iterations of updating cluster features
    #       teu: the temperture of distance matrix
    # output:
    #       cluster_features: shape [B, hw, C]

    B, C, H, W = features.shape

    # initialize the cluster features
    cluster_features = interpolate(features, cluster_features_shape)

    # construct mask to constrain the interactions within local range
    mask = calculate_mask(features.shape, cluster_features_shape)
    mask = (~mask) * 1e16

    features = features.reshape(B, C, -1).permute(0, 2, 1)  # (B, HW, C)
    cluster_features = cluster_features.reshape(B, C, -1).permute(0, 2, 1)  # (B, hw, C)

    for _ in range(num_iters):
        # calculate L2 distance of features and cluster features, the shape distance_matrix is (B, hw, HW)
        distance_matrix = L2_distance(features, cluster_features)
        # mask remote distance through softmax
        distance_matrix += mask
        weights = (-distance_matrix / teu).softmax(dim=1)
        # let the sum of weight of each cluster feature be 1
        weights = weights / weights.sum(dim=2, keepdim=True).clamp_(min=1e-16)
        cluster_features = matrix_product(weights, features)

    return cluster_features
```

Listing 1: PyTorch example of token clustering layer.

```python
def token_reconstruction_layer(cluster_features, features_before_clustering, features_after_clustering, k, teu):
    # args:
    #       cluster_features: shape [B, hw, C]
    #       features_before_clustering: features of alpha-th layer before clustering, shape [B, hw, C]
    #       features_after_clustering: features of alpha-th layer before clustering, shape [B, HW, C]
    #       k: topk parameter
    #       teu: the temperture of weight matrix
    # output:
    #       features: reconstruction features, shape [B, HW, C]

    # calculate L2 distance between features and cluster_features
    distance = L2_distance(features_before_clustering, features_after_clustering)
    weight = exp(-teu * distance)
    # only remain the k weight of the most simliar features, calculating mask
    topk, indices = topk(weight, k=k, dim=2)
    mink = min(topk, dim=-1).values
    mink = mink.unsqueeze(-1).repeat(1, 1, weight.shape[-1])
    mask = greater_or_equal(weight, mink)
    weight = weight * mask

    weight = weight / weight.sum(dim=2, keepdim=True).clamp_(min=1e-16)
    features = matrix_product(weight, cluster_features)

    return features
```

Listing 2: PyTorch example of token reconstruction layer.

Table 2 summarizes the hyper-parameters, including the inserted positions α & α+β of the window token clustering layer & window token reconstruction layer, the number of remaining transformer layers after the token reconstruction layer γ, the total number of transformer layers L, the number of window tokens before clustering $\mathsf{K} \times \mathsf{K}$, the number of window tokens after clustering $\mathsf{k} \times \mathsf{k}$, the number of neighboring pixels λ, the number of EM iterations κ, the temperature value τ, and the number of nearest neighbors k, for Mask2Former and SwinV2-L + HTC++.

C. More Evaluation Details

We illustrate the evaluation details used for measuring the GFLOPs and FPS of different methods in Table 3. We choose the input resolutions for different methods with different backbones according to their official implementations. To illustrate the effectiveness of our method more accurately, we do not include the complexity and latency brought by the especially heavy detection heads or segmentation heads within Mask2Former and SwinV2-L + HTC++. For example, the GFLOPs of

SwinV2-L backbone accounts for only 56.7% of the whole model, therefore, we only report the GFLOPs and FPS improvements of our method over the backbone.

D. Comparison with EViT [3] on Dense Prediction

To demonstrate the advantage of our approach over the representative method that is originally designed for the image classification tasks, i.e., EViT [3], we report the detailed comparison results in Figure 3. The original EViT propose to identify and only keep the top $\rho\%$ tokens according to their attention scores relative to the `[class]` token. Specifically, we follow the official implementations to insert the token identification module into the 8-th, 14-th, and 20-th layer of ViT-L/16 (with 24 layers in total) to decrease the number of tokens by (1-$\rho\%$), respectively. We report the results of EViT by choosing $\rho\%$=60%/70%/80%/90% in Figure 3. Accordingly, we can see that our method significantly outperforms EViT across various GFLOPs & FPS settings when evaluating without either re-training or fine-tuning.

The EViT can not be used for dense prediction directly, as it only keeps around $21.6\% \sim 72.9\%$ of the tokens at last. To reconstruct the missed token representations over the abandoned positions, we apply two different strategies, including (i) reusing the representations before the corresponding token identification module, and (ii) using our token reconstruction layer to reconstruct the missed token representations according to Figure 2a. We empirically find the first strategy achieves much worse results, thus choosing the second strategy by default.

E. Adapting DynamicViT [6] for Dense Prediction

To adapt DynamicViT for dense prediction tasks, we propose to add multiple token reconstruction layers to reconstruct high-resolution representations from the selected low-resolution representations iteratively. Figure 2 (b) presents more details of the overall framework. We also report the comparison results in Table 4.

F. Comparison with Clustered Attention [9], ACT [10], and SMRF [2]

We illustrate the key differences between our approach and the existing clustered attention approaches [9, 10, 2] the following two aspects: (i) These clustering attention methods perform clustering within each multi-head self-attention layer (MHSA) independently while our approach only performs clustering once with the token clustering layer and refines the clustered representations with the following transformer layers. Therefore, our approach introduces a much smaller additional overhead caused by the clustering operation. (ii) These clustering attention methods only reduce the computation cost of each MHSA layer equipped with clustering attention as they maintain the high-resolution representations outside the MHSA layers while Our approach can reduce the computation cost of both MHSA layers and feed-forward network (FFN) layers after the token clustering layer. We further summarize their detailed differences and the experimental comparison resultswith ACT [10](without retraining) in Table 5 and Table 6, respectively.

According to the results in Table 6, we can see that (i) ACT also achieves strong performance without retraining, (ii) our approach is a better choice considering the trade-off between performance and FPS & GFLOPs, e.g., our method achieves close performance as ACT (51.32 vs. 51.38) while running 70% faster (9.1 vs. 5.3) and saving more than 35% GFLOPs (388.2 vs. 614.7).

G. Visualization

We first present the visual comparison results of our approach in Figure 4a, which shows three different configurations over Segmenter+ViT-L/16 achieve 32.13%/48.21%/51.32% when setting the cluster size $\mathrm{h} \times \mathrm{w}$ as 8×8/16×16/24×24, respectively.

Then, we visualize both the original feature maps and the clustering feature maps in Figure 4b. Accordingly, we can see that the clustering feature maps, based on our token clustering layer, well maintain the overall structure information carried in the original high-resolution feature maps.

Last, to verify the redundancy in the tokens of vision transformer, we visualize the attention maps of neighboring tokens in Figure 5.

References

[1] Bowen Cheng, Ishan Misra, Alexander G. Schwing, Alexander Kirillov, and Rohit Girdhar. Masked-attention mask transformer for universal image segmentation. 2022.

[2] Giannis Daras, Nikita Kitaev, Augustus Odena, and Alexandros G Dimakis. Smyrf-efficient attention using asymmetric clustering. *NeurIPS*, 33:6476–6489, 2020.

[3] Youwei Liang, GE Chongjian, Zhan Tong, Yibing Song, Jue Wang, and Pengtao Xie. Evit: Expediting vision transformers via token reorganizations. In *International Conference on Learning Representations*, 2022.

[4] Ze Liu, Han Hu, Yutong Lin, Zhuliang Yao, Zhenda Xie, Yixuan Wei, Jia Ning, Yue Cao, Zheng Zhang, Li Dong, et al. Swin transformer v2: Scaling up capacity and resolution. *arXiv preprint arXiv:2111.09883*, 2021.

[5] René Ranftl, Alexey Bochkovskiy, and Vladlen Koltun. Vision transformers for dense prediction. In *ICCV*, pages 12179–12188, 2021.

[6] Yongming Rao, Wenliang Zhao, Benlin Liu, Jiwen Lu, Jie Zhou, and Cho-Jui Hsieh. Dynamicvit: Efficient vision transformers with dynamic token sparsification. *arXiv preprint arXiv:2106.02034*, 2021.

[7] Mannat Singh, Laura Gustafson, Aaron Adcock, Vinicius de Freitas Reis, Bugra Gedik, Raj Prateek Kosaraju, Dhruv Mahajan, Ross Girshick, Piotr Dollár, and Laurens van der Maaten. Revisiting weakly supervised pre-training of visual perception models, 2022.

[8] Robin Strudel, Ricardo Garcia, Ivan Laptev, and Cordelia Schmid. Segmenter: Transformer for semantic segmentation. *arXiv preprint arXiv:2105.05633*, 2021.

[9] Apoorv Vyas, Angelos Katharopoulos, and François Fleuret. Fast transformers with clustered attention. *NeurIPS*, 33, 2020.

[10] Minghang Zheng, Peng Gao, Renrui Zhang, Kunchang Li, Xiaogang Wang, Hongsheng Li, and Hao Dong. End-to-end object detection with adaptive clustering transformer. *arXiv preprint arXiv:2011.09315*, 2020.

Table 1: Illustrating the hyper-parameter settings used for Segmenter, DPT, and SWAG.

Method	Backbone	Dataset	α	$\alpha+\beta$	γ	L	$\frac{\mathsf{H}}{\mathsf{P}} \times \frac{\mathsf{W}}{\mathsf{P}}$	$\mathsf{h} \times \mathsf{w}$	λ	κ	τ	k
Segmenter [8]	ViT-L/16	ADE20K	10	24	0	24	40×40	28×28	5×5	5	50	20
		Cityscapes	12				48×48	32×32				
		PASCAL-Context	14				30×30	15×15				
DPT [5]	R50+ViT-B/16	KITTI	2	12	0	12	76×22	28×28	5×5	5	5	20
		NYUv2	3				40×30	16×16	7×7	5	10	50
SWAG [7]	ViT-H/14	ImageNet-1K	8	32	0	32	37×37	25×25	7×7	5	1	20
	ViT-L/16		8	24	0	24	32×32	22×22	9×9	5	1	20

Table 2: Illustrating the hyper-parameter settings used for Mask2Former and SwinV2-L + HTC++.

Method	Backbone	Dataset	α	$\alpha+\beta$	γ	L	$\mathsf{K} \times \mathsf{K}$	$\mathsf{k} \times \mathsf{k}$	λ	κ	τ	k
Mask2Former [1]	Swin-L	COCO (panoptic seg.)	10	22	2	24	12×12	8×8	7×7	5	20	10
		ADE20K (semantic seg.)	8						5×5	5	100	10
		COCO (instance seg.)	12						11×11	5	100	60
SwinV2-L + HTC++ [4]	SwinV2-L	COCO (object det.)	12	22	2	24	32×32	23×23	5×5	5	33	20

Table 3: Illustrating the hyper-parameter settings used for measuring FPS and GFLOPs.

Method	Backbone	with Head	Dataset	Input resolution
Segmenter [8]	ViT-L/16	✓	ADE20K	640×640
			Cityscapes	768×768
			PASCAL-Context	480×480
DPT [5]	R50+ViT-B/16	✓	KITTI	1216×352
			NYUv2	640×480
SWAG [7]	ViT-H/14	✓	ImageNet-1K	518×518
	ViT-L/16			512×512
Mask2Former [1]	Swin-L	✗	COCO (panoptic seg.)	1152×1152
			ADE20K (semantic seg.)	1152×1152
			COCO (instance seg.)	1152×1152
SwinV2-L + HTC++ [4]	SwinV2-L	✗	COCO (object det.)	1024×1024

Table 4: Comparison to parametric methods based on Segmenter [8].

Dataset	Method	Parametric	Fine-Tuning	GFLOPs	mIoU
ADE20K	Dynamic ViT ($\rho = 0.7$)	✓	✓	455.6	45.62
	Dynamic ViT ($\rho = 0.8$)	✓	✓	513.3	47.89
	Dynamic ViT ($\rho = 0.9$)	✓	✓	583.0	50.42
	Ours ($\mathrm{h} \times \mathrm{w} = 16 \times 16$)	✗	✗	315.1	48.21
	Ours ($\mathrm{h} \times \mathrm{w} = 20 \times 20$)	✗	✗	347.2	50.17
	Ours ($\mathrm{h} \times \mathrm{w} = 24 \times 24$)	✗	✗	388.2	51.32

Table 5: Illustrating the differences between clustered attention [9], ACT [10], SMRF [2], and our approach.

Cluster method	query	key-value	FFN	#clustering layers
Clustered Attention [9]	✓	✗	✗	# MHSA layers
ACT [10]	✓	✗	✗	# MHSA layers
SMRF [2]	✓	✓	✗	# MHSA layers
Ours	✓	✓	✓	1

Table 6: Comparison results with ACT [10].

Cluster method	FPS	GFLOPs	mIoU
Segmenter+ViT-B/16	6.2	659.0	51.82
Segmenter+ViT-B/16+Ours(h×w=24×24)	9.1	388.2	51.32
Segmenter+ViT-B/16+Ours(h×w=28×28)	8.8	438.9	51.56
Segmenter+ViT-B/16+ACT(#query-hashes=16)	5.8	578.7	48.12
Segmenter+ViT-B/16+ACT(#query-hashes=24)	5.3	614.7	51.38
Segmenter+ViT-B/16+ACT(#query-hashes=32)	5.0	638.2	51.64

(a) Adapting EViT for Dense Prediction

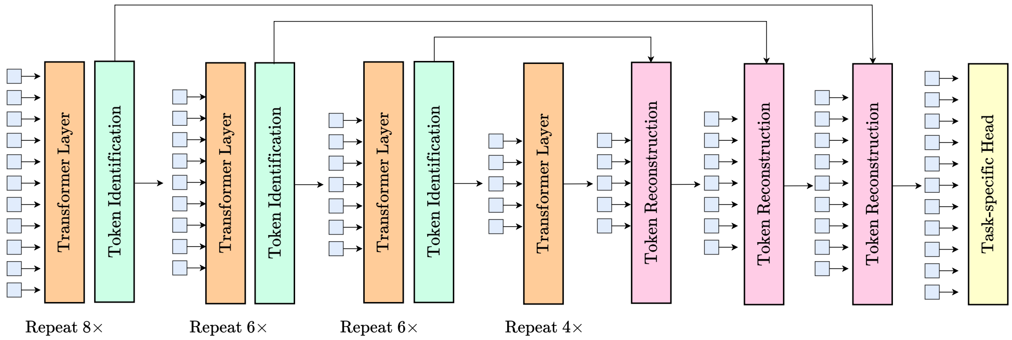

(b) Adapting DynamicViT for Dense Prediction

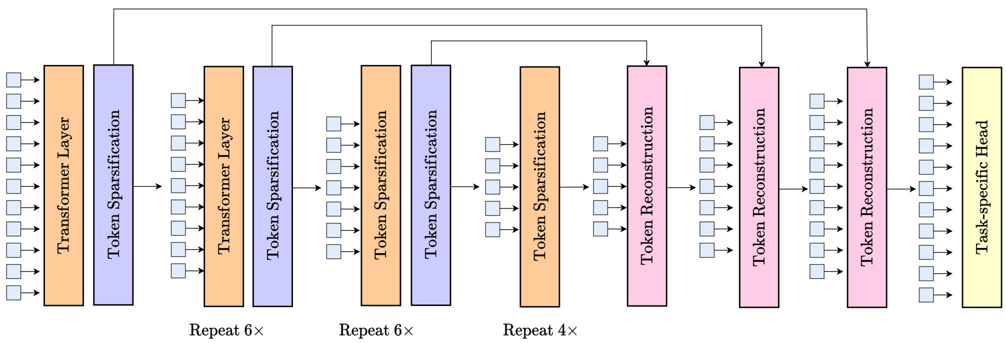

Figure 2: Illustrating how to adapt the EViT [3] and DynamicViT [6] for dense prediction based on ViT-L/16 with 24 transformer layers. Following the proposed token reconstruction scheme, we estimate the semantic relations based on the representations before each token identification layer [3] or token sparsification layer [6].

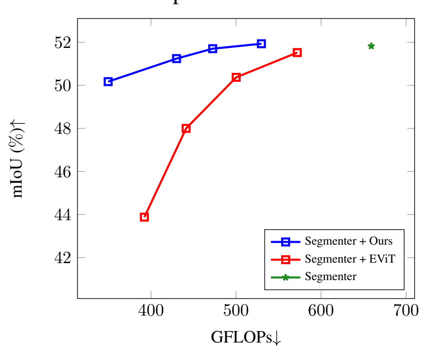

(a) mIoU vs. GFLOPs on ADE20K

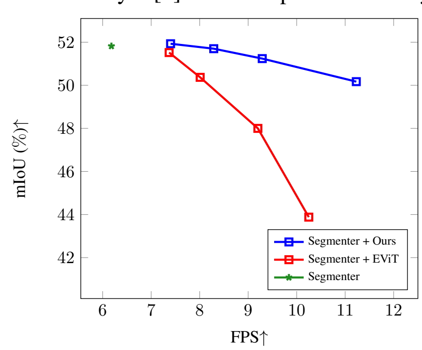

(b) mIoU vs. FPS on ADE20K

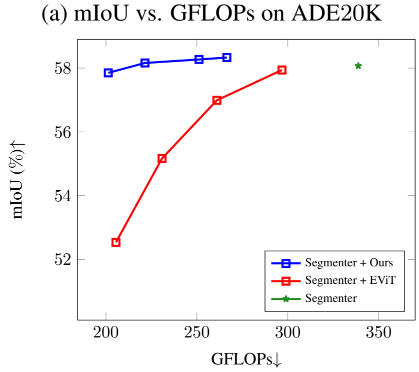

(c) mIoU vs. GFLOPs on PASCAL-Context

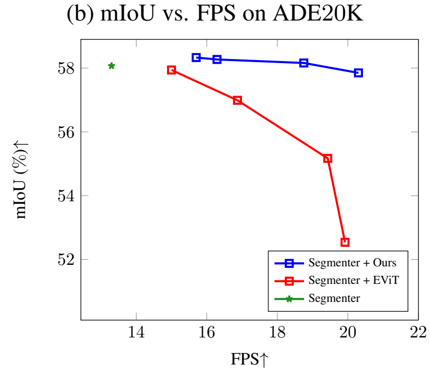

(d) mIoU vs. FPS on PASCAL-Context

Figure 3: Comparison with EViT [3] on ADE20K and PASCAL-Context semantic segmentation task based on Segmenter with ViT-L/16. ↑ and ↓ represent higher is better and lower is better respectively.

(a) ADE20K example segmentation results of our approach with $\mathrm{h} \times \mathrm{w}$ as 8×8, 16×16, 24×24 on the left three columns, respectively. The right-most column shows the results of the original Segmenter+ViT-L/16. We can see that our approach achieves consistently better segmentation results with increasing clustered output resolutions from left to right.

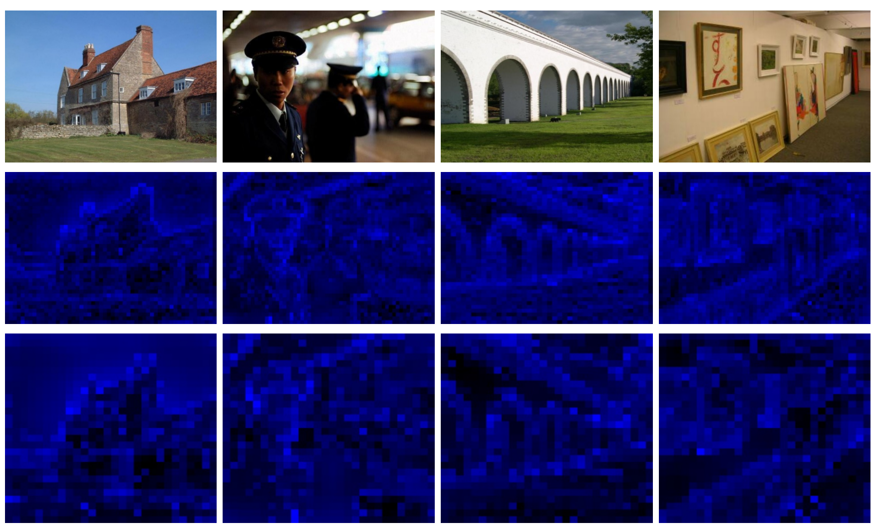

(b) ADE20K example visualization of the original feature maps (2-ed row) and the clustering feature maps (3-rd row). We can see that the clustering feature maps still maintain the structure information presented in the original high-resolution feature maps, thus showing the potential benefits of our token clustering scheme.

Figure 4: Visualizations of segmentation results in (a) and feature maps in (b). We choose Segmenter+ViT-L/16 on ADE20K to generate the above segmentation results and the feature map visualizations.

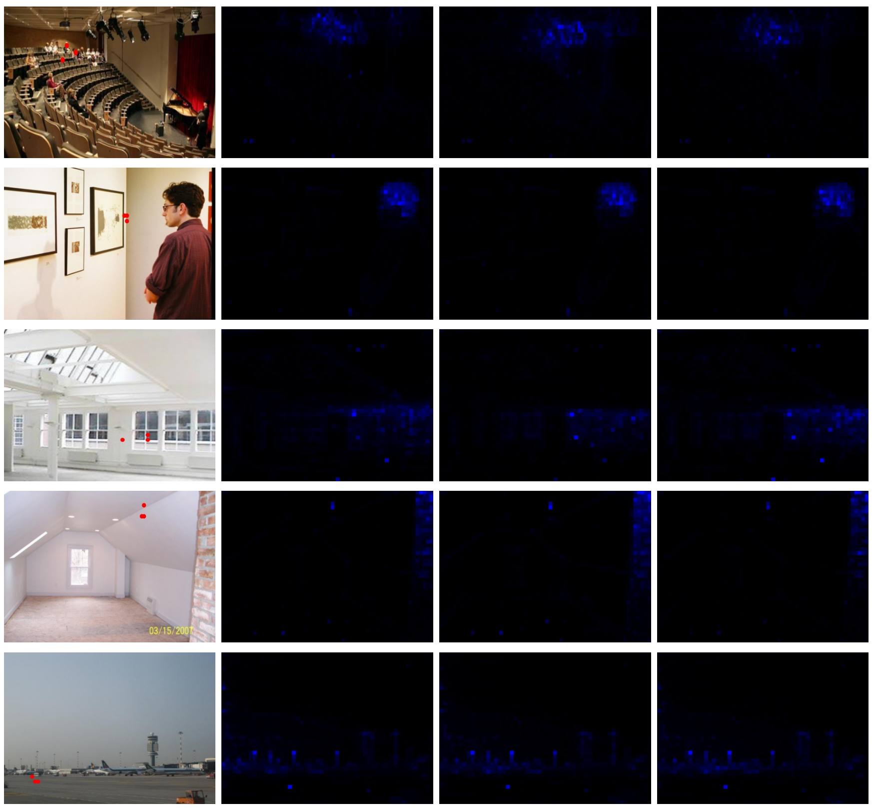

Figure 5: Visualizations of the attention maps of neighboring sampled positions. We mark the sampled positions with red point markers. We can see that the neighboring positions share highly similar attention maps, which matches the redundancy observation in the Adaptive Clustering Transformer (ACT) [10].